Letters in Applied NanoBioScience
Platinum Open Access Journal (ISSN: 2284-6808)

Article
Volume 9, Issue 4, 2020, 1459 - 1466
https://doi.org/10.33263/LIANBS94.14591466

Semiempirical Molecular Modeling Analyses for Graphene/Nickel Oxide Nanocomposite

Hend A. Ezzat [1], Islam Gomaa [2], Alaa El-Din A. Gawad [3], Osama Osman [4], Abdel Aziz Mahmoud [4], Mohamed S. Abdel-Aal [4], Hanan Elhaes [5], Medhat A. Ibrahim [4,*]

1 Nano Technology Unit, Solar and Space Research Department, National Research Institute of Astronomy and Geophysics (Nano NRIAG), 11421 Helwan, Cairo, Egypt
2 Holding Company for water and wastewater, Ismailia, Egypt
3 Biophysics and Laser Science Unit, Research Institute of Ophthalmology, 2, Al-Ahram St, Giza 12111, Egypt
4 Molecular Spectroscopy and Modeling Unit, Spectroscopy Department, National Research Centre, 33 El-Bohouth St., 12622 Dokki, Giza, Egypt
5 Physics Department, Faculty of Women for Arts, Science and Education, Ain Shams University, 11757 Cairo, Egypt
* Correspondence: medahmed6@yahoo.com;

Scopus Author ID 8641587100
Received: 22.07.2020; Revised: 11.08.2020; Accepted: 12.08.2020; Published: 15.08.2020

Abstract: Graphene metal oxide composite show applications in many areas according to their excellent electronic properties. Accordingly, graphene was subjected to interaction with NiO as adsorbing and a complex state. Semiempirical quantum mechanical calculations at PM6 was used to study the total energy, the final heat of formation, ionization energy, total dipole moment as well the charge distribution of the surface of graphene metal oxide composite. Calculated data indicated that graphene symmetry is changed into the C1 point group, forming stable composites with NiO that the complex composites were more stable compared with adsorb state composites. The change in the partial charge of graphene is responsible for the change in total dipole moment and hence affecting the increase in the reactivity of graphene/nickel oxide composite.

Keywords: NiO; Total dipole moment; symmetry and PM6.

1. Introduction

Carbon-based materials are widely used in many applications owing to their low cost, high surface-area-to-volume ratio, high electrical conductivity, and high thermal stability [1-2]. It could be used for storing charges electrodes by means of physical adsorption, which renders high power density and long cycle life rather than battery-grade materials [3]. Functionalized carbon-based materials could be achieved with the help of metal oxides. For storage materials, graphene/metal oxides are considered as redox-active and have been utilized as an efficient energy storage electrode [4-5]. Among metal oxides NiO is considered as a redox transition metal active material, characterized by its abundance, low price, thermal and chemical stability, it is also known as eco-friendly which in turn makes it easy for disposal. It is reported that graphene supported metal oxide, especially those in the nanoscale, show the affection of metal oxide graphene surface [6-7]. Graphene/metal oxide shows potential applications according to their unique properties, which are previously reported [8-12]. Among the wide range of applications, it was applied in biology [13], catalysis [14], imaging [15], and sensors [16]. NiO is classified as an antiferromagnetic semiconductor with an energy bandgap

of about 3.6 eV [17]. However, it is characterized by its highly electronic properties, but it shows the impact in different applications covering other fields such as biological applications. As it shows both antibacterial and antifungal activities [18], this, in turn, allows researchers to apply it as an anticancer agent [19]. According to the unique electronic properties of G/NiO and a wide range of applications, researchers devote their work to experimental characterizations of such composite. Many research works are then devoted to elucidating the structural, vibrational, surface, electrical, electrochemical, and thermal properties of G/NiO [20-24]. Molecular modeling with several levels of theories and/or different softcodes provides important physical, chemical, and biological parameters for molecular systems [25-26]. These parameters are important for understanding the structure and behaviors of many systems and molecules in different fields of applications [27-30]. It was an attempt to correlate reactivity of the drug with the physical parameters such as total dipole moment, HOMO/LUMO band gab energy together with molecular electrostatic potential as stated earlier for the reactivity of chemical structures [31-36]. Understanding the effect of metal oxide on the electronic properties of graphene leads to continuous developments in the molecular modeling methods to follow up on the expected changes. So that, graphene was interacted with NiO through adsorb state than through the complex. Also, the interaction took place once through O-atom of the NiO then through Ni-atom. The studied model molecules are then subjected to PM6 model to study some physical parameters indicating the effect of NiO on graphene.

2. Materials and Methods

2.1. Calculation details.

All the studied model molecules were calculated using SCIGRESS software [37] at Molecular Spectroscopy and Modeling Unit, Spectroscopy Department, National Research Centre, Egypt. Each model molecule is subjected to semiempirical calculations at PM6 [38] method to calculate the physical parameters and estimate the charge transfer then the total dipole moment of the studied model molecules. For comparison with a higher level of theory, graphene is subjected to calculation with DFT at B3LYP/3-21g* [39-41] with Gaussian 09 program [42] at Molecular Spectroscopy and Modeling Unit, Spectroscopy Department, National Research Centre, Egypt.

3. Results and Discussion

The first step in this work is to introduce the steps conducted for building the studied model molecules. As indicated in figure 1, sheet consists of 46 carbon atoms is chosen as a model molecule for graphene.

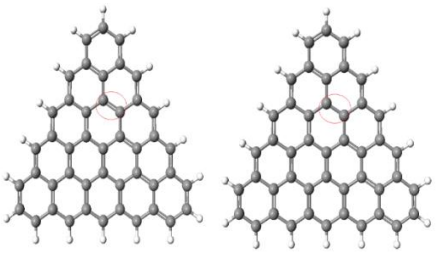

Figure 1. Studied model molecule for graphene, which is consists of 46 carbon atoms, the labeled atoms indicated the C=C bond which is broken to form C-C, then 2NiO interact with graphene throughout these two atoms.

One of the bonds between C=C is broken, then two molecules of NiO is introduced as complex in two ways once through O to form G/2ONi then through Ni to form G/2NiO as indicated in figure 2, a, b. Throughout the same C=C. The same is repeated without broken of bonds to form G/2ONi and G/2NiO as adsorb state, as indicated in figure 2 c, d.

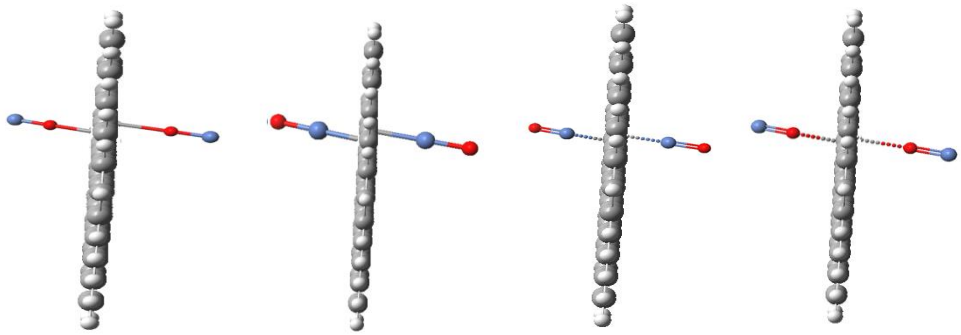

a- b- c- d-

Figure 2. Studied model molecules for graphene G, which is interacted as a complex with NiO throughout oxygen, then nickel to form a- G/2NiO, b- G/2ONi then to form c- G/2NiO, c- G/2ONi.

The studied model molecules will be subjected to PM6 calculations that need some kind of verification and/or validation. In order to validate the PM6 mode, a comparison with a higher level of theory is conducted. In order to verify the data obtained by PM6, compassion is carried out with a higher level of theory. Accordingly, PM6 is compared with DFT:B3LYP/3-21g*, as indicated in figure 3. A listed in table 1 some parameters calculated, such as the bond distance C-C, bond angle C-C-C, HOMO/LUMO bandgap energy, and finally, the total dipole moment. These parameters are calculated from the first derivative. The results show comparable values, while PM6 has the advantage of calculation within a reasonable time as it is not a high-cost method.

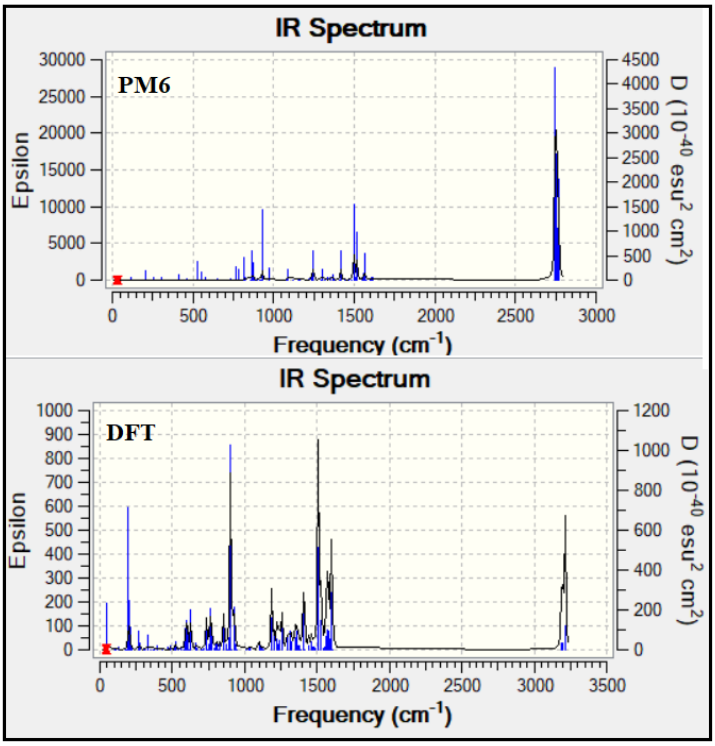

Figure 3. Comparison between calculated IR spectra of graphene at PM6 as indicated in (a) and at DFT:B3LYP/3-21g* as indicated in (b).

Table 1. Comparison between calculated parameters which calculated at PM6 and DFT:B3LYP/3-21g*.

Calculated parameter	PM6	DFT:B3LYP/3-21g*
C-C Å	1.4265	1.4202
C-C-C º	120.078	120.000
HOMO/LUMO eV	0.3940	0.3010
Total dipole moment	1.274	0.900

Another comparison could be through the second derivative as one compares between the calculated IR for two methods, as seen in figure 3. Figure 3 presents the two spectra for graphene at PM6 and DFT:B3LYP/3-21g*. Although both spectra are nearly the same that corresponding to PM6 is shifted and not in coincidence with a higher level of theory.

This is maybe due to the effect of electron correlation, which is not concluded in the PM6 but included in DFT method [43]. Correlating the data for physical parameters in table 1 with the vibrational frequencies in figure 3, one can conclude that PM6 method gives reasonable physical data in an appropriate time, while vibrational data is not so accurate. Accordingly, in this study, the studied model molecules will be calculated with PM6.

Table 2. PM6 calculated total energy (eV), the final heat of formation (KCal), electronic energy (eV), ionization potential, total dipole moment as Debye (eV), point group, for G, C46/2NiO and C46/2ONi as adsorb state than as a complex state.

Descriptors		Adsorb state		Complex state	
	G	C46/2NiO	C46/2ONi	C46/2NiO	C46/2 ONi
Molecular weight	570.648	724.099	724.099	724.099	724.099
Total energy	-5871.767	-7481.769	-7477.3930	-7485.3649	-7486.444
Final heat of formation	265.244	327.259	428.182	244.344	219.458
Point group	D3h	C1	C1	C1	C1
Ionization potential	6.456	7.177	6.707	1.198	0.245
Total dipole moment	1.274	10.708	1.476	7.891	4.105

We are going to compare each parameter for G/NiO with the same parameter for G. As indicated in table 2. The molecular weight was 570.648 then increased to be 724.099 for all composites, whatever the interaction adsorb or complex.

Regarding the calculated total energy, it was 5871.767 eV, which is lower than those for G/NiO in both adsorb and complex states. This is an indication that the studied G/NiO composite is stable. For the calculated final heat of formation for G was 265.24379 Kcal, then it became higher corresponding to adsorb state then decreased correspondingly to complex state. This means that the formation of G/NiO as the complex is more stable than the formation of G/NiO as adsorb state. The molecular point group for G was D3h, which is the symmetry of a tricapped trigonal prism, this is really a good description for the slab of graphene used as a model molecule in this work. As far as graphene interacts with CaO, D3h is changed into C1 for all the studied composites, which an indication that the composites became with no symmetry. This could be an indication of the deformation that happened as a result of the composite formation, at least at this level of theory. This also may be a limitation for the studied PM6 method. The ionization potential for G was 6.456 eV increased for G/NiO as adsorb state then dramatically decreased correspondingly to complex state.

Finally, the total dipole moment is calculated for G as 1.274 Debye then increased as 10.708 Debye C46/2NiO (adsorb state), 7.891 Debye for C46/2NiO (complex state), and finally was 1.476 Debye (complex state), for C46/2ONi (adsorb state). The dipole moment is a good descriptor for the chemical reactivity of the graphene as well as its composites as well as other molecular systems, as stated earlier [44-45].

As stated in building model molecule one of the C=C is broken then we follow up the changes in two carbon atoms. Accordingly, the results in table 3 are presented for those two

atoms. For G, the charge was -0.032417 and 0.032116. the number of electrons also for G was 4.0324 and 3.9679. These electrons distributed as (1.08407, 2.94835) and (1.09544, 2.87245) for s-Pop and p-Pop for each carbon atom. Comparing the same values for G/NiO it is clear that the existence of metal oxide is changing the charge partially which in turn changing the electron configurations also this is maybe the reason for changing the values of the total dipole moment indicated in table 1 and subsequently induced chemical interaction in terms the dipole moment. In terms of the calculated total dipole moment, the composite C46/2NiO as adsorbing and complex state are most reactive as compared with the other two composites.

Although PM6 is relative as compared with a higher level of theory, but still of concern for many applications as indicated in the present work. This finding is in good agreement with the previous findings [46-49].

Table 3. PM6 calculated total charge, a number of electrons, with distribution in s-Pop and p-Pop for G/2CaO and G/2OCa as adsorb state G/2CaO and G/2OCa as complex.

Calculated quantity		Adsorb state		Complex	
	G	C46/2NiO	C46/2ONi	C46/2NiO	C46/2 ONi
Charge	-0.032417	-0.116303	0.101361	0.014081	0.263516
	0.032116	-0.125846	-0.097267	-0.217273	0.300649
No. of electrons	4.0324	4.1163	3.8986	3.9859	3.7365
	3.9679	4.1258	4.0973	4.2173	3.6994
s-Pop	1.08407	1.08040	1.08675	1.08339	1.10510
	1.09544	1.08819	1.09230	1.10496	1.10442
p-Pop	2.94835	3.03590	2.81189	2.90253	2.63138
	2.87245	3.03765	3.00497	3.11231	2.59490

4. Conclusions

Graphene is subjected to interaction through adsorbing and complex states with NiO forming four composites. The semiempirical calculation at PM6 indicated that deformation took place while the studied composites are stable with higher stabilities for the complex state as compared with adsorb state. The existence of NiO induces a change in the charge partially, which in turn changed the total dipole moment. The total dipole moment is responsible for the chemical reactivity of the studied composites.

Although PM6 is relatively low computational cost with reasonable accuracy, but still potentially valid method for predicting some properties such as charge, ionization potential with comparable results with ab initio methods, while predicting IR frequencies, requires a higher level of theory

Funding

This research received no external funding.

Acknowledgments

This research has no acknowledgment.

Conflicts of Interest

The authors declare no conflict of interest.

References

1. Agudosi, E.S.; Abdullah, E.C.; Numan, A.; Mubarak, N.M.; Aid, S.R.; Benages-Vilau, R.; Gómez-Romero, P.; Khalid, M.; Omar, N. Fabrication of 3D binder-free graphene NiO electrode for highly stable supercapattery. *Sci. Rep.* **2020,** *10*, https://doi.org/10.1038/s41598-020-68067-2.
2. Najib, S.; Erdem, E. Current progress achieved in novel materials for supercapacitor electrodes: Mini review. *Nanoscale Adv.* **2019,** *1*, 2817–2827, https://doi.org/10.1039/C9NA00345B.
3. Shao, H., Padmanathan, N.; McNulty, D.; O'Dwyer, C.; Razeeb, K.M. Supercapattery based on binder-free Co3(PO4)2·8H2O multilayer nano/microflakes on nickel foam. *ACS Appl. Mater. Inter.* **2016,** *8*, 28592–28598, https://doi.org/10.1021/acsami.6b08354.
4. Kate, R.S.; Khalate, S.A.; Deokate, R.J. Overview of nanostructured metal oxides and pure nickel oxide (NiO) electrodes for supercapacitors: A review. *J. Alloy. Compd.* **2018,** *734*, 89–111, https://doi.org/10.1016/j.jallcom.2017.10.262.
5. Xiang, Y.; Yang, Z.; Wang, S.; Shahriar, Md.; Hossain, A.; Yu, J.; Kumar, N.A.; Yamauch, Y. Pseudocapacitive behavior of the Fe2O3 anode and its contribution to high reversible capacity in lithium ion batteries. *Nanoscale* **2018,** *10*, 18010–8018, https://doi.org/10.1039/C8NR04871A.
6. Moussa, S.O.; Panchakarla, L.S.; Ho, M.Q.; El-Shall, M.S. Graphene-supported, iron-based nanoparticles for catalytic production of liquid hydrocarbons from synthesis gas: the role of the graphene support in comparison with carbon nanotubes. *ACS Catal.* **2014**, *4*, 535-545, https://doi.org/10.1021/cs4010198.
7. Bagheri, S.; Mansouri, N.; Aghaie, E. Phosphorene: a new competitor for graphene. *Int. J. Hydrog. Energ.* **2016**, *41*, 4085-4095, https://doi.org/10.1016/j.ijhydene.2016.01.034.
8. Lingamdinne, L.P.; Koduru, J.R.; Karri, R.R. Acomprehensive review of applications of magnetic graphene oxide based nanocomposites for sustainable water purification. *J. Environ. Manage.* **2019**, *231*, 622-634, https://doi.org/10.1016/j.jenvman.2018.10.063
9. Lingamdinne, L.P.; Koduru, J.R.; Choi, Y.L.; Chang, Y.Y., Yang, J.K. Studies on removal of Pb(II) and Cr(III) using graphene oxide based inverse spinel nickel ferrite nano-composite as sorbent. *Hydrometallurgy* **2016**, *165*, 64-72, https://doi.org/10.1016/j.hydromet.2015.11.005.
10. Posa, V.R.; Annavaram, V.; Koduru, J.R.; Ammireddy, V.R.; Somala, A.R. Graphene-ZnO nanocomposite for highly efficient photocatalytic degradation of methyl orange dye under solar light irradiation. *Korean J. Chem. Eng.* **2016**, *33*, 456-464, https://doi.org/10.1007/s11814-015-0145-4.
11. Wang, D.; Yan, W.; Vijapur, S.H.; Botte, G.G. Electrochemically reduced graphene oxide–nickel nanocomposites for urea electrolysis. *Electrochim. Acta* **2013**, *89*, 732-736, https://doi.org/10.1016/j.electacta.2012.11.046
12. Lingamdinne, L.P.; Koduru, J.R.; Changa Y.Y.; Karri R.R. Process optimization and adsorption modeling of Pb(II) on nickel ferrite-reduced graphene oxide nano-composite. *J. Mol. Liq.* **2018**, *250*, 202-211, https://doi.org/10.1016/j.molliq.2017.11.174.
13. Archana, S.; Kumar, K. Y.; Jayanna, B.K.; Olivera, Sh.; Anand, A.; Prashanth, M.K.; Muralidhara, H.B. Versatile graphene oxide decorated by star shaped zinc oxide nanocomposites with superior adsorption capacity and antimicrobial activity. *J. Sci-Adv. Mat. Dev.* **2018**, *3*, 167-174, https://doi.org/10.1016/j.jsamd.2018.02.002.
14. Navalon, S.; Dhakshinamoorthy, A.; Alvaro, M.; Garcia, H. Carbocatalysis by graphene-based materials. *Chem. Rev.* **2014**, *114*, 6179-6212, https://doi.org/10.1021/cr4007347
15. Luo, B.; Zhi, L. Design and construction of three dimensional graphene-based composites for lithium ion battery applications, *Energ. Environ. Sci.* **2015**, *8*, 456-477, https://doi.org/10.1039/C4EE02578D.
16. Mansouri, N.; Babadi, A.A.; Bagheri, S.; Hamid, S.B.A. Immobilization of glucose oxidase on 3D graphene thin film: novel glucose bioanalytical sensing platform. *Int. J. Hydrog. Energ.* **2017**, *42*, 1337-1343, https://doi.org/10.1016/j.ijhydene.2016.10.002.
17. Gandhi, A.C.; Wu, S.Y. Strong deep-level-emission photoluminescence in NiO nanoparticles. *Nanomaterials* **2017,** *7*, https://doi.org/10.3390/nano7080231.
18. Helana, V.; Princea, J.J.; Al-Dhabib, N.A.; Arasub, M.V.; Ayeshamariamc, A.; Madhumithad, G.; Roopan, S.M.; Jayachandran, M. Neem leaves mediated preparation of NiO nanoparticles and its magnetization, coercivity and antibacterial analysis. *Results Phys.* **2016**, *6*, 712-718, https://doi.org/10.1016/j.rinp.2016.10.005.
19. Mohameda, K.; Zinea, K.; Fahimaa, K.; Abdelfattahc, E.; Sharifudind, S.; Duduku, K. NiO nanoparticles induce cytotoxicity mediated through ROS generation and impairing the antioxidant defense in the human lung epithelial cells (A549): preventive effect of Pistacia lentiscus essential oil. *Toxicol. Rep.* **2018**, *5*, 480-488, https://doi.org/10.1016/j.toxrep.2018.03.012.
20. Wang, G.; Zhang, L.; Zhang, J. A review of electrode materials for electrochemical supercapacitors. *Chem. Soc. Rev.* **2012,** *41*, 797–828, https://doi.org/10.1039/c1cs15060j.
21. Yao, S.; Zhu, Y. Nanomaterial-enabled stretchable conductors: Strategies, materials and devices. *Adv. Mater.* **2015,** *27*, 1480–1511, https://doi.org/10.1002/adma.201404446.
22. Atif, R.; Shyha, I.; Inam, F. Mechanical, Thermal, and Electrical Properties of Graphene-Epoxy Nanocomposites—A Review. *Polymers (Basel)* **2016**, *8*, https://doi.org/10.3390/polym8080281.

23. Zeng, G.; Li, W.; Ci, S. Highly Dispersed NiO Nanoparticles Decorating graphene Nanosheets for Non-enzymatic Glucose Sensor and Biofuel Cell. *Sci. Rep.* **2016,** *6*, https://doi.org/10.1038/srep36454.
24. Afzali, M.; Mostafavi, A.; Shamspur, T. Decoration of graphene oxide with NiO@polypyrrole core-shell nanoparticles for the sensitive and selective electrochemical determination of piceatannol in grape skin and urine samples. *Talanta.* **2019**, *196*, 92-99, https://doi.org/10.1016/j.talanta.2018.12.029.
25. Ibrahim, M.; Abd-El-Aal, M. Spectroscopic study of the Interaction of Heavy Metals with Organic Acid. Int. J. Environ. Pollut. **2008,** *35*, 99-110, https://doi.org/10.1504/IJEP.2008.021134.
26. Ibrahim, M.; Osman, O. Spectroscopic Analyses of Cellulose: Fourier Transform Infrared and Molecular Modelling Study. *J. Comput. Theor. Nanosci.* **2009,** *6*, 1054–1058, https://doi.org/10.1166/jctn.2009.1143.
27. Ibrahim, M. Molecular Modelling and FTIR Study for K, Na, Ca and Mg Coordination with Organic Acid. *J. Comput. Theor. Nanosci.* **2009,** *6*, 682–685, https://doi.org/10.1166/jctn.2009.1094.
28. Muzaffar, S.; Imtiaz, S.; Ali, S.M. Demonstrating accuracy of the proposed protocol for structure elucidation of cyclodextrin inclusion complexes by validation using DFT studies. *J. Mol. Struct.* **2020,** *12175*, https://doi.org/10.1016/j.molstruc.2020.128419.
29. Ignaczak, A.; Orszański, Ł.; Adamiak, M.; Olejniczak, A.B. Comparative DFT study of inclusion complexes of thymidine-carborane conjugate with β-cyclodextrin and heptakis(2,6-O-dimethyl)-β-cyclodextrin in water. *J. Mol. Liq.* **2020**, *315*, https://doi.org/10.1016/j.molliq.2020.113767.
30. Ezzat, H.A.; Hegazy, M.A.; Nada N.A.; Ibrahim, M.A. Effect of Nano Metal Oxides on the Electronic Properties of Cellulose, Chitosan and Sodium Alginate. *Biointerface Res. Appl.* **2019**, *9*, 4143-4149, https://doi.org/10.33263/BRIAC94.143149.
31. Abdelsalam, H.; Saroka, V.A.; Ali, M.; Teleb, N.H.; Elhaes, H.; Ibrahim, M.A. Stability and electronic properties of edge functionalized silicene quantum dots: A first principles study. *Physica E* **2019**, *108*, 339–346, https://doi.org/10.1016/j.physe.2018.07.022.
32. Grenni, P.; Caracciolo, A.B.; Mariani, L.; Cardoni, M.; Riccucci, C.; Elhaes, H.; Ibrahim, M.A. Effectiveness of a new green technology for metal removal from contaminated water. *MICROCHEM. J.* **2019**, *147*, 1010-1020, https://doi.org/10.1016/j.microc.2019.04.026.
33. Shkoor, M.; Mehanna, H.; Shabana, A.; Farhat, T.; Bani-Yaseen, A.D. Experimental and DFT/TD-DFT computational investigations of the solvent effect on the spectral properties of nitro substituted pyridino[3,4-c]coumarins. *J. Mol. Liq.* **2020**, *3131*, https://doi.org/10.1016/j.molliq.2020.113509.
34. Badry, R.; Radwan, S. H.; Ezzat, D.; Ezzat, H.; Elhaes, H.; Ibrahim, M. Study of the Electronic Properties of Graphene Oxide/(PANi/Teflon). *Biointerface Res. Appl.* **2020**, *10*, 6926–6935, https://doi.org/10.33263/BRIAC106.69266935.
35. Bayoumy, A.M.; Refaat, A.; Yahia, I.S.; Zahran, H.Y.; Elhaes, H.; Ibrahim, M.A.; Shkir, M. Functionalization of Graphene Quantum Dots (GQDs) with Chitosan Biopolymer for Biophysical Applications. *Opt Quant. Electron.* **2020**, *52*, https://doi.org/10.1007/s11082-019-2134-z.
36. Omar, A.; Ezzat, H.; Elhaes, H.; Ibrahim, M.A. Molecular Modeling Analyses for Modified Biopolymers. *Biointerface Res. Appl.* **2021**, *11*, 7847-7859, https://doi.org/10.33263/BRIAC111.78477859.
37. MO-G Version 1.1A, Fujitsu Limited, Tokyo, Japan **2008**.
38. Stewart, J.J.P. Optimization of parameters for semiempirical methods V: Modification of NDDO approximations and application to 70 elements. *J. Mol. Mod.* **2007**, *13*, 1173-1213, https://doi.org/10.1007/s00894-007-0233-4.
39. Becke, A.D. Density-functional thermochemistry. III. The role of exact exchange. *J. Chem. Phys.***1993**, *98*, 5648–5652, https://doi.org/10.1063/1.464913.
40. Lee, C.; Yang, W.; Parr, R.G. Development of the Colic-Salvetti correlation-energy formula into a functional of the electron density. *Phys. Rev. B* **1988**, 37, 785-789, https://doi.org/10.1103/PhysRevB.37.785.
41. Miehlich, B.; Savin, A.; Stoll, H.; Preuss, H. Results Obtained with the Correlation Energy Density Functionals of Becke and Lee, Yang and Parr. *Chem. Phys. Lett.* **1989**, *157*, 200–206, https://doi.org/10.1016/0009-2614(89)87234-3.
42. Frisch, M.; Trucks, G.; Schlegel, H.; Scuseria, G.; Robb, M.; Cheeseman, J.; Scalmani, G.; Barone, V.; Mennucci, B.J.I. Gaussian, Inc., Wallingford CT,**2010**.
43. Foresman, J.B. Chapter 14-Ab initio techniques in chemistry: interpretation and visualization. In: *What every chemist should know about computing*. Ed. Swift, M.L.; Zielinski, T.J. Acs Books, Washington, D.C. **1996**.
44. Ibrahim, M.; El-Haes, H. Computational Spectroscopic Study of Copper, Cadmium, Lead and Zinc Interactions in the Environment. *Int. J. Environ. Pollut.* **2005**, *23*, 417-424, http://dx.doi.org/10.1504/IJEP.2005.007604.
45. Ibrahim, M.; Mahmoud, A.A. Computational Notes on the Reactivity of some Functional Groups. *J. Comput. Theor. Nanosci.* **2009**, *6*, 1523-1526, https://doi.org/10.1166/jctn.2009.1205.
46. Al-Bagawi, A.H.; Bayoumy, A.M.; Ibrahim, M.A. Molecular Modeling Analyses for Graphene Functionalized with Fe3O4 and NiO. *Heliyon* **2020**, *6*, https://doi.org/10.1016/j.heliyon.2020.e04456.
47. Miličević, A.; Miletić, G.I.; Jovanović, I.N. Electrochemical oxidation of flavonoids: PM6 and DFT for elucidating electronic changes and modelling oxidation potential. *J. Mol. Liq.* **2019**, *2851*, 551-556, https://doi.org/10.1016/j.molliq.2019.04.128.

48. Miličević, A.; Miletić, G.I.; Jovanović, I.N. Electrochemical oxidation of flavonoids: PM6 and DFT for elucidating electronic changes and modelling oxidation potential (part II). *J. Mol. Liq.* **2019**, *295*, https://doi.org/10.1016/j.molliq.2019.111730.
49. Issa, Y.M.; Abdel-Maksoud, G.; Ibrahim, M.; Magdy, M. A combination of analytical methods to evaluate the effect of humidity aging on the painting materials of icon models. *Vib. Spectrosc*. **2020**, *107*, https://doi.org/10.1016/j.vibspec.2019.103010.